Journal of Fluorine Chemistry 131 (2010) 1218–1224

Contents lists available at ScienceDirect

Journal of Fluorine Chemistry

journal homepage: www.elsevier.com/locate/fluor

Halogen-bonded and interpenetrated networks through the self-assembly of diiodoperfluoroarene and tetrapyridyl tectons

Michele Baldrighi [a], Pierangelo Metrangolo [a,b,**], Franck Meyer [a], Tullio Pilati [c], Davide Proserpio [d], Giuseppe Resnati [a,b,c,*], Giancarlo Terraneo [a,b]

[a] NFMLab - D.C.M.I.C. "Giulio Natta", Politecnico di Milano, Via L. Mancinelli 7, 20131 Milan, Italy
[b] CNST - IIT@POLIMI, Politecnico di Milano, Via G. Pascoli 70/3, 20133 Milan, Italy
[c] C.N.R. - I.S.T.M., University of Milan, Via C. Golgi 19, 20133 Milan, Italy
[d] Department of Structural Chemistry and Inorganic Stereochemistry, University of Milan, 21, via Venezian, 20133 Milan, Italy

ARTICLE INFO

Article history:
Received 18 April 2010
Received in revised form 28 May 2010
Accepted 1 June 2010
Available online 10 June 2010

Keywords:
Diiodoperfluoroarenes
Self-assembly
Halogen bonding
Interpenetrated networks
Supramolecular chemistry

ABSTRACT

The formation of two organic interpenetrated networks on halogen bonding driven self-assembly of diiodoperfluorarenes with tetrapyridyl tectons is described. Both architectures exhibit two-dimensional square 4^4 networks; with either a 2-fold interpenetration of class IIa or a 3-fold interpenetration of class Ia. Diiodoperfluoroarenes are proven robust tectons in the design of interpenetrated networks based on the *expansion* strategy.

1. Introduction

The design and self-assembly of interpenetrated networks is an important topic in supramolecular chemistry. Interpenetrating networks can be thought of as polymeric analogues of molecular catenanes and rotaxanes, and they involve the intimate entanglement of two or more polymeric networks [1]. Defining feature of interpenetration is the condition that the entanglement of the topological nets is such that, although there is no direct connection between the networks, they cannot be separated (in a topological sense) without requiring the breaking of network connections. Infinite 2D and 3D networks with a variety of interpenetration modes have been built [2].

Much of the recent progress in this area is based on tailor-made building blocks, either organic or metal–organic, and their self-assembly was based on hydrogen bonding (HB) and metal–ligand coordination. Quite often organic interpenetrated networks are formed in the pursuit of porous lattice structures when tetradentate tectons are connected by organic linkers. The geometric and chemical attributes of linkers allow for producing conveniently open framework topologies. When the 2D or 3D primary networks, formed *via* HB or metal–ligand coordination, possess open structures with large voids, the starting building modules can be accommodated within these voids, namely interpenetration is present in the overall crystal architecture and reduces the unoccupied space within the crystal lattice.

As a complement of HB, halogen bonding (XB), namely any noncovalent interactions involving halogen atoms as acceptors of electronic density, is emerging as a new item in the supramolecular toolbox [3]. During the last decade, this interaction has ensured the deliberate construction of supramolecular architectures involving ionic or neutral tectons [4] and showing interesting properties in diverse areas of Materials Science [5]. Few examples of halogen-bonded interpenetrated networks have been reported in the literature so far [6]. However, XB has proven to exert an unprecedented level of control over the formation of entangled structures. This level of control is related to the remarkably high directionality of the XB which preferentially develops on the extension of the C-halogen covalent bond, the stronger XBs resulting in the more linear arrangements.

* Corresponding author at: NFMLab - D.C.M.I.C. "Giulio Natta", Politecnico di Milano, Via L. Mancinelli 7, 20131 Milan, Italy. Tel.: +39 02 2399 3032; fax: +39 02 2399 3180.
** Co-corresponding author at: NFMLab - D.C.M.I.C. "Giulio Natta", Politecnico di Milano, Via L. Mancinelli 7, 20131 Milan, Italy. Tel.: +39 02 2399 3041; fax: +39 02 2399 3180.
E-mail addresses: pierangelo.metrangolo@polimi.it (P. Metrangolo), giuseppe.resnati@polimi.it (G. Resnati).

0022-1139/$ – see front matter © 2010 Elsevier B.V. All rights reserved.
doi:10.1016/j.jfluchem.2010.06.001

The XB directionality is related to the fact that the electron density around halogen atoms is anisotropically distributed and in the elongation of the C-halogen bond a region of positive electrostatic potential is present (σ-hole) [7]. This positive region accounts for the directionality of the approach of the high electron density site of the electron donor to the halogen atom.

As a consequence of the high polarizability of the iodine atom and the ability of fluorine to boost the electron-acceptor potential of iodine, diiodoperfluoroarenes are particularly effective and telechelic XB-donors. Moreover, we have already demonstrated that the geometry of the XB-donor sites on starting diiodoperfluoroarene modules strongly influences the geometry of the noncovalent co-polymers obtained on self-assembly with XB-acceptors. For instance, when 1,4-diiodotetrafluorobenzene is co-crystallized with 4,4′-bipyridine (XB-acceptor), linear 1D infinite chains are obtained wherein the two modules alternate thanks to the presence of N···I XBs [8]. On the other hand, when 1,2-diiodotetrafluorobenzene is co-crystallized with the same XB-acceptor, infinite chains wherein the two modules alternate are obtained once more, and the 60° angle of the XB-donor sites on the perfluoroarene ring translates into the wave-like arrangement of the infinite chain [9]. For these reasons, diiodoperfluoroarenes can be considered very reliable XB-tectons in geometry-based crystal engineering.

As to interpenetrated networks sustained by XB, we have recently described the self-assembly of a three-component system made up of the kryptand K.2.2.2, KI, and α,ω-diiodoperfluoroalkanes. The scavenging of potassium cations by the K.2.2.2 allowed for obtaining naked iodide anions that were able to bind three different perfluorinated modules resulting into corrugated honeycomb-like (6,3) networks. When 1,6-diiodoperfluorohexane and 1,8-diiodoperfluorooctane were used, the obtained (6,3) networks were large enough to give rise to the fascinating and rare interpenetration pattern of Borromean links [10].

The rigid rod-like behaviour of perfluoroalkyl chains and the remarkable directionality of XB were also employed for the deliberate construction of highly interpenetrated neutral networks by self-assembly of diiodoperfluorolkanes with tetradentate XB-acceptors. Specifically, the self-assembly of tetrapyridylpentaerythritol with 1,6-diiodoperfluorohexane and 1,8-diiodoperfluorooctane afforded architectures exhibiting 2D square 4^4 networks with 4-fold and 5-fold interpenetration of class IIIa and class Ia, respectively. On the other hand, when tetrapyridylpentaerythritol self-assembles with 1,4-diiodoperfluorobutane or with tetrakis(4-iodotetrafluorophenyl)pentaerythritol, a rare 8-fold diamondoid network of class Ia or a notable 10-fold diamondoid network were formed. This last interpenetration is one of the highest degrees of interpenetration reported to date for organic structures [6a].

With these results in mind, we decided to investigate the use of differently sized diiodoperfluoroarenes as telechelic and XB-based

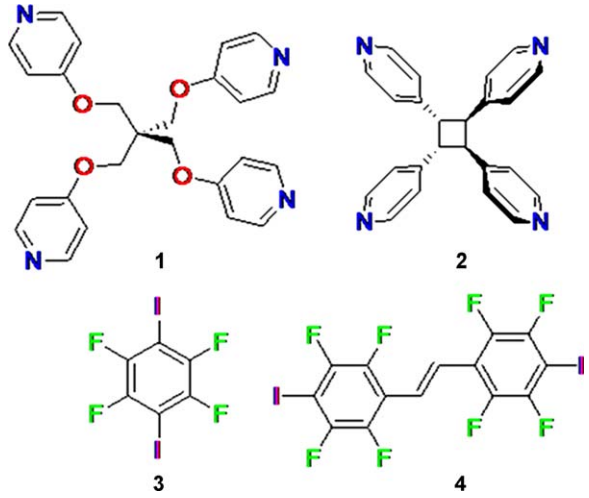

Scheme 1. XB-acceptor (**1** and **2**) and XB-donor (**3** and **4**) modules involved in the self-assembly processes.

linkers of tetrapyridyl tectons. The selected building blocks functionalized with four pyridyl rings are the tetrapyridylpentaerythritol **1** (TPPE) and the tetrakis(4-pyridyl)cyclobutane **2** (TPCB). Few interpenetrated organic networks have been obtained from the tetrapyridyl XB-acceptors **1** and a 3-fold interpenetrated organometallic network was formed when a Zn^{2+} salt was bound to two TPCB and two dipyridylethylene molecules [11].

1,4-Diiodotetrafluorobenzene **3** was chosen as XB-donor linker. Considering that the directionality of XB can translate the geometry of the starting modules into the topology of the obtained supramolecular architectures (Scheme 1), the simplest way to enlarge the cavities of the primary network formed on self-assembly of tectons with a given geometry was to increase the length of one, or both, the starting modules. In other words, our concept was to tune the size of the cavity of the primary networks by changing the size of the compounding modules. 4,4′-Diiodooctafluorostilbene **4** was thus prepared with the aim to obtain networks with larger cavities allowing for higher interpenetration. The use of the diiodoperfluoroarenes **3** and **4** in the formation of interpenetrated networks gives also the possibility to study how the remarkable tendency of perfluoroarenes to give rise to π···π stacking interactions influences the network topologies and interpenetration modes [12].

Specifically, the pentaerythritol-based module **1** was self-assembled with the XB-donor module **4** and the tetrapyridylcyclobutane **2** with the benzene derivative **3**. The obtained structures **5** and **6** both exhibit two-dimensional square 4^4 networks, the former having a 3-fold interpenetration of class Ia and the latter a 2-fold interpenetration of class IIa (Scheme 2).

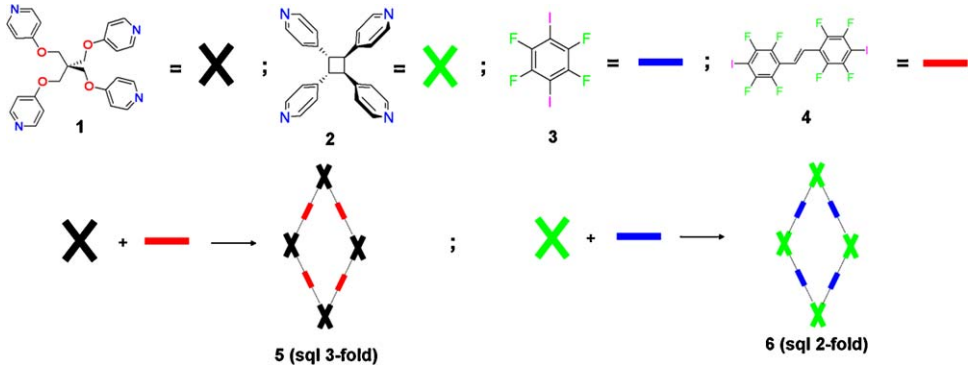

Scheme 2. Formation of square networks **5** and **6** upon self-assembly of modules **1** and **4**, and **2** and **3**, respectively.

2. Results and discussion

2.1. Synthesis of starting building blocks

Entangled systems are frequently formed from tetradentate tectons, the molecular geometry of which is translated into the topology of the obtained framework thanks to the use of rigid organic linkers which connect the tetradentate tectons and increase their spacing in a process which is often referred to as *expansion* [13]. Tetradentate tectons based on pentaerythritol and cyclobutane cores appeared to be a particularly attractive starting building block as several architectures incorporating this tetradentate core have been reported [14]. Modules **1** and **2** were thus used in this study. The tetrakis(4-pyridyl)pentaerythritol (**1**) was prepared by an improved synthetic protocol starting from pentaerythritol (**7**) and 4-chloropyridine (**8**) in the presence of *t*BuOK in DMSO (Scheme 3). The *rctt*-tetrakis(4-pyridyl)cyclobutane (**2**) was synthesized by irradiating at 300 nm the co-crystal obtained from *trans*-1,2-bis(4-pyridyl)ethylene and tetrakis(4-iodotetrafluoro-phenyl)pentaerythritol [15]. We have already reported that the supramolecular control exerted by the crystal packing over the regio- and stereochemistry of the [2 + 2] photochemical cycloaddition secures the formation of **2** in quantitative chemical and stereochemical yields.

Our previous studies demonstrated that differently sized diiodoperfluoroalkanes were particularly successful organic linkers in the *expansion* strategy to highly interpenetrated networks [6a]. In this paper we decided to explore if diiodoperfluoroarenes are equally effective linkers. 1,4-Diiodotetrafluorobenzene **3** is commercially available and 4,4′-diiodooctafluorostilbene **4** was synthesized by a two step sequence (Scheme 4). First a Wittig reaction between triphenyl-(2,3,5,6-tetrafluorobenzyl)phosphonium bromide (**9**) and 2,3,5,6-tetrafluorobenzaldehyde (**10**) gave the *trans*-1,2-bis-(1,2,4,5-tetrafluorophenyl)-ethylene (**11**) which was diiodinated to the target product **4** with *n*-BuLi/I_2 (94% overall yield).

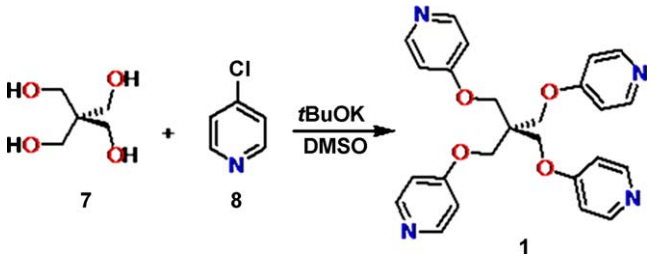

Scheme 3. Synthesis of XB-acceptor module **1**.

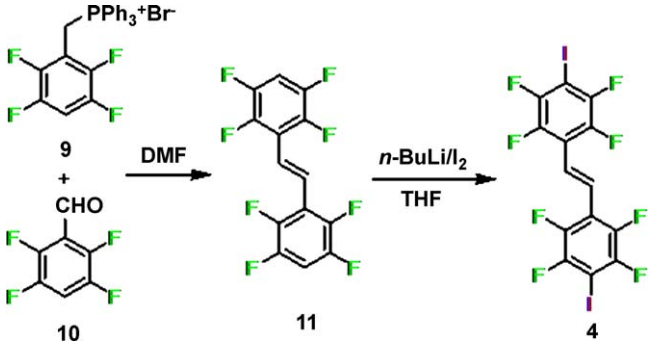

Scheme 4. Synthesis of XB-donor module **4**.

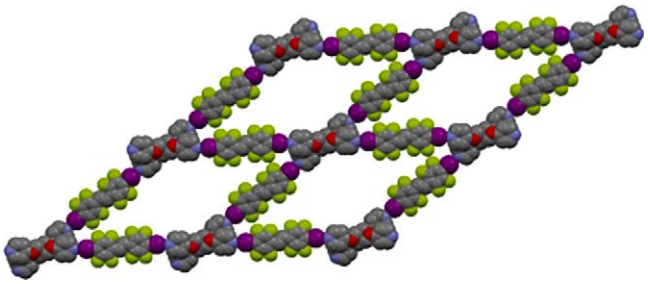

Fig. 1. Schematic representation (spacefill style by using Mercury 2.3 [17]) of the 2D square network formed on self-assembly of molecules **1** and **4**. The network given by molecules **A** and **C** is reported, molecules **B** and **D** give a very similar network. H atoms have been omitted for clarity; colour codes: grey, carbon; yellow-green, fluorine; blue, nitrogen; red, oxygen; purple, iodine. (For interpretation of the references to color in this figure legend, the reader is referred to the web version of the article.)

2.2. Synthesis and crystal structure analysis of the complex 5

The co-crystal **5** was obtained upon slow and isothermal evaporation at room temperature of a 9:1 MeOH/CH_2Cl_2 solution containing the tetrapyridyl compound **1** and the diiodinated module **4** in a 1:2 ratio. The co-crystal **5** melts at 242–244 °C, namely much higher than the starting compounds (**1** melts at 198 °C, and **4** melts at 207–210 °C) thus confirming the expected formation of a new crystalline species, rather than a mechanical mixture of starting compounds.

Single crystal X-ray diffraction analyses of **5** shows [16] that the pentaerythrytol derivative **1** and the diiodinated module **4** are present in a 1:2 ratio. N···I XBs are largely responsible for the self-assembly of the complementary modules **1** and **4** to give co-crystal **5**. N···I distances span the range of 2.785–2.819 Å (approximately 80% of the sum of Van der Waals radii of N and I) and N···I–C angles are 175.3–178.8°, consistent with the directionality typical for XBs.

The topology of the primary network formed by the self-assembly of **1** and **4** is a nice example of the paradigm of the *expansion* of a tetratopic starting module by a linear linker. Each pentaerythritol derivative **1** behaves as a tetratopic XB-acceptor and each stilbene module **4** functions as a linear and ditopic XB-donor spacing two tetradentate pentaerythritol derivatives **1**. 2D, parallel, and square networks having a 4^4 topology are formed and they are compounded by rhombic meshes having a side length of 31.208 Å (Fig. 1).

The asymmetric unit of the co-crystal **5** consists in two molecules of **4**, indicated here as **A** and **B**, and two half molecules of **1**, indicated as **C** and **D**, both with the mass centre on a crystallographic 2-fold symmetry axis (Fig. 2). Due to this asymmetric unit, two independent and parallel 2D square networks containing molecules **A** and **C**, and **B** and **D**, respectively, are obtained. The couples of molecule **A**, **B** and **C**, **D** have very similar conformations, and the directionality of the XB transfer this similarity to the two independent and parallel 2D square networks, closely resembling each other.

The overall crystal packing is formed by alternating layers containing either **A**, **C** or **B**, **D** molecules. Each layer result from the interpenetration of three different square networks with the shortest interpenetration vector [1 0 0] of 19.707 Å (Figs. 3 and 4).

Finally, it may be worth noting that few short contacts other than N···I XBs contribute to the crystal packing of the complex **5**. Modules **1** and **4** of the same layer interact each other through a net of H···F HBs (the shorter being 2.44 Å), and modules **1** and **4** of adjacent layers loosely interact through weak π···π stacking involving perfluoroarene and pyridine rings (centroid-centroid distance of 3.754 Å).

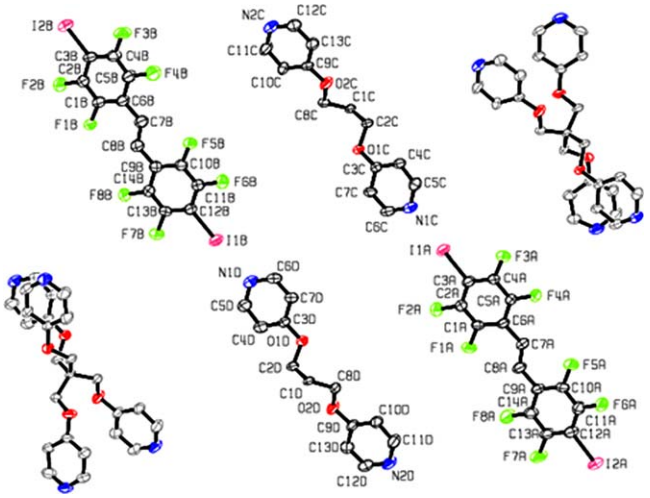

Fig. 2. Asymmetric unit of co-crystal **5** (by using ORTEP-3 [18]) with numbering scheme and atomic displacement parameters (ADPs) at 50% probability level. Two complete TPPE molecules **C** and **D** are reported at the corners. H atoms have been omitted for clarity; colour codes: grey, carbon; yellow-green, fluorine; blue, nitrogen; red, oxygen; purple, iodine. (For interpretation of the references to color in this figure legend, the reader is referred to the web version of the article.)

2.3. Synthesis and crystal structure analysis of the complex 6

Single crystals of the complex **6** were prepared by isothermal (r.t.) evaporation of a methanol solution containing the two starting modules **2** and **3** in a 1:2 ratio. Good-quality single crystals in the form of colourless prisms were obtained after 3 days. The crystals melted at 190–193 °C, much higher than the mean value of the starting compounds melting points (218–220 °C and 108–110 °C for **2** and **3**, respectively).

The single crystal X-ray diffraction analysis reveals the crystal structure of **6** presents several similarities to **5**. The starting modules **2** and **3** are present in a 1:2 ratio (Fig. 5), they behave as a tetratopic XB-acceptor and as a linear ditopic XB-donor, respectively, and the diiodinated module **3** functions as a linear spacer expanding the tetradentate module **2**.

Here too N···I XBs are largely responsible for the complementary modules self-assembly [20]. N···I distances span the range

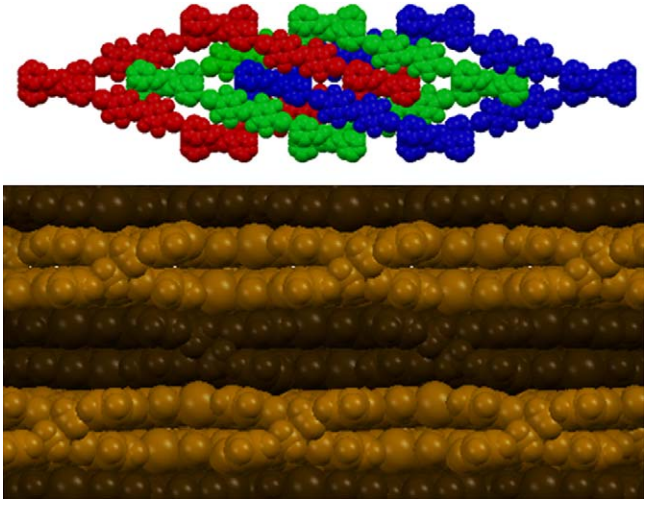

Fig. 3. Top: view along the *c*-axis of 3-fold interpenetration for one layer formed by **A** and **C** molecules. Molecules **B** and **D** give very similar interpenetrating meshes. Bottom: view along the *b*-axis of the alternating layers formed by **A**, **C** molecules (bright brown) and **B**, **D** molecules (dark brown) in co-crystal **5**. (For interpretation of the references to color in this figure legend, the reader is referred to the web version of the article.)

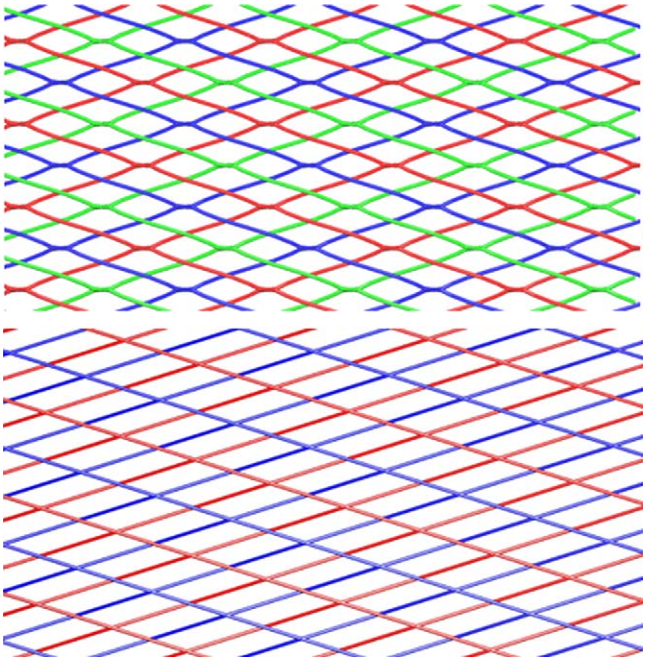

Fig. 4. Top: schematic representation (by using TOPOS 4.0 [19]) of the 3-fold interpenetrated network of **5**. Colours as in Fig. 3, top. Bottom: TOPOS schematic representation of the 2-fold interpenetrated networks of **6**. Colours as Fig. 7, top. (For interpretation of the references to color in this figure legend, the reader is referred to the web version of the article.)

2.794–3.040 Å (the shortest one corresponding to approximately 79% of the sum of Van der Waals radii) and N···I–C angles are 162.2–177.7°, once again perfectly consistent with the preferred directionality of the XB. Also in complex **5**, N···I XBs produce 2D square networks having a 4^4 topology (Fig. 6) and the overall crystal packing consists in loosely interacting layers formed on interpenetration of the square networks having a 4^4 topology (Fig. 7). However, the meshes of the square networks of **6** are parallelograms having sides of 21.051 and 21.681 Å and the layers present in the overall crystal packing are formed thanks to a 2-fold interpenetration of class IIa [21] (interpenetration vector along [1 0 1]) (Figs. 4 and 7).

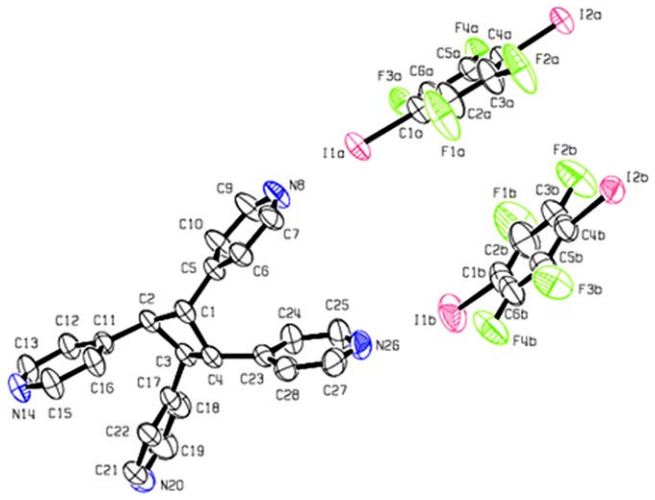

Fig. 5. Asymmetric unit in the crystal structure of **6** (by using ORTEP-3 [18]) with numering scheme and ADPs at 50% probability level. H atoms have been omitted for clarity; colour codes: grey, carbon; yellow-green, fluorine; blue, nitrogen; purple, iodine. (For interpretation of the references to color in this figure legend, the reader is referred to the web version of the article.)

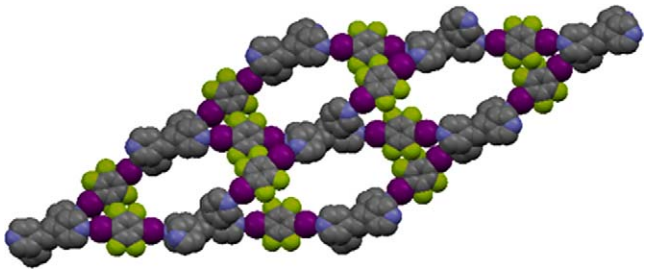

Fig. 6. Schematic representation (spacefill style by using Mercury 2.3 [17]) of the 2D square network formed on self-assembly of molecules **2** and **3**, forming the complex **6**. H atoms have been omitted for clarity; colour codes: grey, carbon; yellow-green, fluorine; blue, nitrogen; purple, iodine. (For interpretation of the references to color in this figure legend, the reader is referred to the web version of the article.)

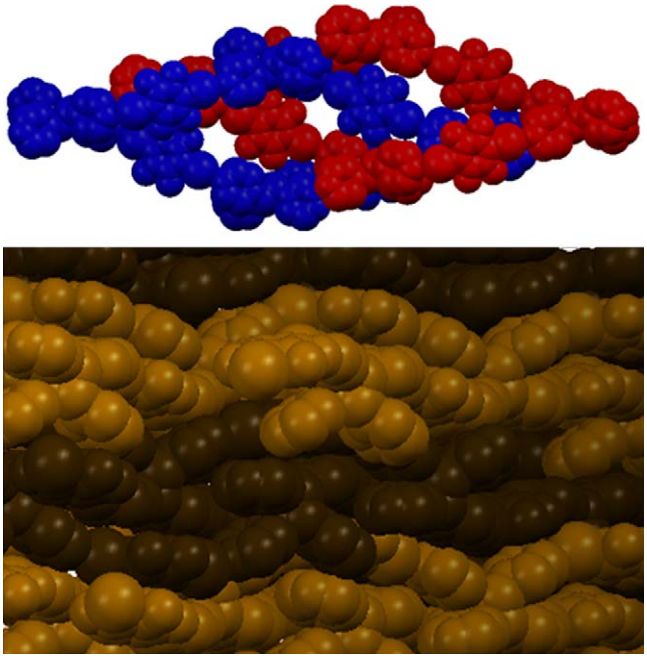

Fig. 7. Top: schematic view of the 2-fold interpenetration for one layer in co-crystal **6**. Bottom: overall crystal packing in **6** formed by loosely interacting layers.

3. Conclusions

This paper described how the supramolecular architecture **5** is composed of alternating layers of independent 2D square networks with a 3-fold interpenetration. The individual nets in the layer are related by a unique vector of translation and are classified as class Ia. Similarly, the overall crystal packing of the co-crystal **6** is formed by layers of parallel square networks with a 2-fold interpenetration of class IIa.

The rhombs of **5** are 591 $Å^2$ and the parallelograms of **6** are 358 $Å^2$, namely the network meshes in **5** are larger than in **6**. This diversity is related to the different sizes of starting module: The distances between adjacent nitrogens of the same molecule in the same mesh are 11.9 and 5.6 Å for tetrapyridylpentaerythritol **1** and 9.6, and 5.3 Å for tetrapyridylcyclobutane **2**, the distances between adjacent iodines in the same molecule in the same mesh are 13.7 Å for diiodostilbene **4** and 7.0 Å for diiodobenzene **3**. The directionality of the XB can transfer these molecular differences to the supramolecular networks thanks to the ability of diiodoperfluoroarenes to work cleanly as XB-donor spacers of XB-acceptors.

The larger voids present in **5** allow for higher interpenetration. Diiodoperfluoroarenes are thus proven robust tectons in the design of interpenetrated networks based on the *expansion* strategy [13]. Clearly the remarkable tendency of perfluoroarenes to give rise to $\pi\cdots\pi$ stacking interactions does not influence their reliability in geometry-based crystal engineering.

In summary, XB-donor and -acceptor modules with similar geometries and different sizes afford self-assembled networks with similar topologies and different sizes. The larger modules afford more extended networks and the resulting larger voids allow for a higher interpenetration. The generality of this design principle is still under study by co-crystallizing **1** with **3** and **2** with **4** and using 2,4,6-triiodotrifluorobenzene as tridentate XB-donor spacers of bi- and tridentate XB-acceptors.

4. Experimental

4.1. Materials and methods

Commercial HPLC-grade solvents were used without further purification. Starting materials were purchased from Sigma–Aldrich, Acros Organics, and Apollo Scientific. The mass spectra were recorded on a GC–MS AGILENT GC-MSD5975. ^{1}H NMR and ^{19}F NMR spectra were recorded at ambient temperature with a Bruker AV500 spectrometer. Unless otherwise stated, $CDCl_3$ was used as both solvent and internal standard in ^{1}H NMR spectra. For ^{19}F NMR spectra, $CDCl_3$ was used as solvent and $CFCl_3$ as internal standard. All chemical shift values are given in ppm. Melting points were determined with a Reichert instrument by observing the melting and crystallising process through an optical microscope. The photoreaction was carried out in a Rayonet RPR-100 instrument using monochromatic irradiation at λ = 300 nm.

4.2. Tetrakis(4-pyridyl)pentaerythritol (1)

68 mg (0.5 mmol) of pentaerythritol (**7**) and 280 mg (2.5 mmol) of *t*BuOK are stirred in 1 mL of DMSO at room temperature for 40 min. Then, 590 mg (10.4 mmol) of 4-chloropyridine (**8**) diluted in 1 mL of DMSO are added slowly and the reaction is heated at 50 °C. After 24 h, a saturated aqueous solution of NaCl is added, the aqueous layer is extracted 4 times with CH_2Cl_2 and the combined organic layers are dried over Na_2SO_4. After evaporation of the solvent, the crude material is chromatographed on silica gel (240–400 mesh, eluent CH_2Cl_2/MeOH 2:1) to give 200 mg of the tetrakis(4-pyridyl)pentaerythritol (**1**) in 90% yield. mp = 198 °C; ^{1}H NMR: δ 4.47 (8H, s, CH_2), 6.80 (8H, d, J = 6.4 Hz, H arom.), 8.40 (8H, d, J = 6.4 Hz, H arom.); IR: ν_{max} = 3025, 2944, 1598, 1504, 1464, 1424, 1278, 1214, 1025, 842, 816, 654 cm^{-1}.

4.3. Trans-1,2-bis-(1,2,4,5-tetrafluorophenyl)-ethylene (11)

600 mg (1.19 mmol) of triphenyl-(2,3,5,6-tetrafluoro-benzyl)-phosphonium bromide (**9**) and 62 mg (1.54 mmol) of NaH are stirred in 3 mL of DMF for 30 min. 0.15 mL (1.31 mmol) of 2,3,5,6-tetrafluorobenzaldehyde (**10**) are then added to the mixture and the solution is heated at 40 °C. After 3 h, the reaction is poured on H_2O and the white solid is filtered and residue is chromatographied on silica gel (240–400 mesh, eluent *n*-hexane/CH_2Cl_2 4:1) to give 339 mg of *trans*-1,2-bis-(1,2,4,5-tetrafluorophenyl)-ethylene (**11**) in 88% yield. mp = 135–138 °C; ^{1}H NMR: δ 7.03 (2H, m, H arom.), 7.46 (2H, s, CH=CH); ^{19}F NMR: δ = −142.9 (4F, m, CF–C), −139.8 (4F, m, CF–CH); m/z (EI): 324 {$M^{\bullet+}$}.

4.4. Trans-1,2-bis-(2,3,5,6-tetrafluoro-4-iodophenyl)-ethylene (4)

300 mg (0.92 mmol) of perfluorinated olefine derivative **11** is stirred in suspension in 3 mL of THF at −70 °C. 1.73 mL of *n*-BuLi (1.6 M) is added slowly and the mixture is warmed up to room temperature. After 20 mn, 561 mg I_2 (2.21 mmol) is added and the

solution is mixed 25 mn. Then, the reaction is hydrolysed with $Na_2S_2O_3$ sat., the aqueous layer is extracted 3 times with CH_2Cl_2 and the organic phase is dried over Na_2SO_4. After evaporation of the solvent, 503 mg (95% yield) of the compound **4** is recovered in pure form without further purification.

mp = 200–210 °C; ^{1}H NMR: δ 7.44 (2H, s, CH=CH); ^{19}F NMR: δ = −141.5 (4F, m, CF–C), −122.1 (4F, m, CF–CI); *m*/*z* (EI): 526 {$M^{\bullet+}$}.

4.5. Tetrakis(4-pyridyl)cyclobutane 2

TPCB **2** was prepared quantitatively by photocyclization of a complex made of *trans*-1,2-bis(4-pyridyl)ethylene and tetrakis(4-iodotetrafluoro-phenyl)pentaerythritol at 300 nm [15].

mp = 234 °C; ^{1}H NMR: δ 4.47 (4H, s, CH), 6.99 (8H, d, J = 6.0 Hz, H arom.), 8.44 (8H, d, J = 6.0 Hz, CH–N arom.); IR: ν_{max} = 3060, 3024, 2904, 1595, 1551, 1412, 1137, 1068, 992, 814 cm^{-1}.

4.6. Formation of co-crystals 5 and 6

Co-crystals **5** and **6** were obtained by dissolving at room temperature, in a vial of clear borosilicate glass, 1 equiv. of tetrakis(4-pyridyl) derivative (**1** and **2**: 10 mg) and 2 equiv. of fluorinated compound (**3** and **4**) in a mixture MeOH–CH_2Cl_2 for **5** and MeOH for **6**. The open vial was placed in a closed cylindrical wide-mouth bottle containing vaseline oil. The solvent was allowed to partially diffuse at room temperature.

4.7. Co-crystal 5: tetrakis(4-pyridyl)pentaerythritol (1)/1,2-bis-(2,3,5,6-tetrafluoro-4-iodophenyl)-ethylene (4)

11 mg of co-crystal **5** were isolated; mp = 242–244 °C; IR 1,2-bis-(2,3,5,6-tetrafluoro-4-iodophenyl)-ethylene **4**: ν_{max} = 3113, 1471, 1453, 1394, 1333, 956, 796, 602 cm^{-1}. Co-crystal **5**: 3119, 3035, 1593, 1470, 1271, 1208, 1014, 953, 814 cm^{-1}.

4.8. Co-crystal 6: tetrakis(4-pyridyl)cyclobutane (2)/diiodotetrafluorobenzene (3)

9 mg of co-crystal **6** were isolated; mp = 190–193 °C; IR diiodotetrafluorobenzene **3**: ν_{max} = 1457, 1430, 1355, 1214, 939, 757 cm^{-1}. Co-crystal **6**: 3029, 2956, 2849, 1598, 1453, 1414, 937, 822, 752 cm^{-1}.

4.9. Analysis by X-ray diffraction

The **5** and **6** single crystal X-ray structures were collected at 295(3) K with a Bruker KAPPA APEX II with CCDC area detector diffractometer using graphite-monochromated Mo Kα radiation (λ = 0.71069 Å); ω and φ scans; data collection and data reduction were performed with the SMART and SAINT program packages. The structures were solved by *SIR*2002 [22] and refined by *SHELXL*-97 [23] programs. The refinement was carried on by full-matrix least-squares on F^2.

4.9.1. Crystallographic data for 5

$C_{25}H_{24}N_4O_4{\cdot}2(C_{14}H_2F_8I_2)$, M_r = 1596.39, crystal size 0.24 mm × 0.20 mm × 0.15 mm, orthorhombic, space group $C222_1$, a = 19.707(2), b = 20.001(2), c = 27.233(3) Å, V = 10734(2) Å^3, Z = 8, D_c = 1.976 g cm^{-3}, μ(Mo Kα) = 2.428 mm^{-1}, 102,079 data collected, $2\theta_{max}$ = 61.52°, absorption correction based on multiscan procedure (T_{min}/T_{max} = 0.837), R_{ave} = 0.0345, 15925 unique data, 12703 with $I_o > 2\sigma(I_o)$; refined parameters 731, H atoms calculated, final disagreement factors for all/observed reflections $R_w(F^2)$ = 0.0813/0.0753, $R(F)$ = 0.0504/0.0341, goodness-of-fit = 1.077, min/max residues −0.41/1.14 e Å^{-3}.

4.9.2. Crystallographic data for 6

$C_{24}H_{20}N_4{\cdot}2(C_6F_4I_2)$, M_r = 1168.16, crystal size 0.24 mm × 0.20 mm × 0.11 mm, monoclinic, space group $P2_1/n$, a = 14.343(3), b = 14.639(3), c = 18.563(4) Å, β = 101.68(4), V = 3821.0(14) Å^3, Z = 4, D_c = 2.031 g cm^{-3}, μ(Mo Kα) = 3.333 mm^{-1}, 108,808 data collected, $2\theta_{max}$ = 60.00°, absorption correction based on multiscan procedure (T_{min}/T_{max} = 0.803), R_{ave} = 0.0325, 11,151 unique data, 8736 with $I_o > 2\sigma(I_o)$; refined parameters 549, 126 restraints on atomic and thermal parameters of H atoms, final disagreement factors for all/observed reflections $R_w(F^2)$ = 0.0886/0.0801, $R(F)$ = 0.0466/0.0343, goodness-of-fit = 1.009, min/max residues −1.08/1.39 e Å^{-3}.

All crystallographic data (excluding structure factors) were deposited to the Cambridge Crystallographic Data Centre as supplementary publication Nos. CCDC 772762 for (**5**) and CCDC 7727621 for (**6**). Copies of the data can be obtained free of charge on application to CCDC, 2 Union Road, Cambridge CB2 1EZ, UK, e-mail: deposit@ccdc.cam.ac.uk.

Acknowledgments

The financial support from Fondazione Cariplo (Project "New-Generation Fluorinated Materials as Smart Reporter Agents in ^{19}F MRI") and MIUR (Project "Engineering of the Self-assembly of Molecular Functional Materials via Fluorous Interactions") are gratefully acknowledged.

References

[1] (a) S.R. Batten, R. Robson, Angew. Chem. Int. Ed. 37 (1998) 1460–1494, references therein;
(b) http://www.chem.monash.edu.au/staff/sbatten/interpen/index.html;
(c) S.R. Batten, CrystEngComm 3 (2001) 67–73;
(d) I.A. Baburin, V.A. Blatov, L. Carlucci, G. Ciani, D.M. Proserpio, Cryst. Growth Des. 8 (2008) 519–539;
(e) I.A. Baburin, V.A. Blatov, L. Carlucci, G. Ciani, D.M. Proserpio, CrystEngComm 6 (2004) 378–395.
[2] (a) D.R. Turner, S.R. Batten, CrystEngComm 10 (2008) 170–172;
(b) N.R. Kelly, S. Goetz, S.R. Batten, P.E. Kruger, CrystEngComm 10 (2008) 68–78;
(c) S.R. Batten, J. Solid State Chem. 178 (2005) 2475–2479;
(d) H. Adams, S.R. Batten, G.M. Davies, M.B. Duriska, J.C. Jeffery, P. Jensen, J. Lu, G.R. Motson, S.J. Coles, M.B. Hursthouse, M.D. Ward, Dalton Trans. (2005) 1910–1923;
(e) X.-H. Bu, M.-L. Tong, H.-C. Chang, S. Kitagawa, S.R. Batten, Angew. Chem. Int. Ed. 43 (2004) 192–195;
(f) M.-L. Tong, X.-M. Chen, S.R. Batten, J. Am. Chem. Soc. 125 (2003) 16170–16171;
(g) I.A. Baburin, V.A. Blatov, L. Carlucci, G. Ciani, D.M. Proserpio, J. Solid State Chem. 178 (2005) 2471–2493;
(h) L. Carlucci, G. Ciani, D.M. Proserpio, Coord. Chem. Rev. 246 (2003) 247–289.
[3] (a) P. Metrangolo, G. Resnati, Science 321 (2008) 918;
(b) P. Metrangolo, G. Resnati, Chem. Eur. J. 7 (2001) 2511–2519;
(c) P. Metrangolo, H. Neukirch, T. Pilati, G. Resnati, Acc. Chem. Res. 38 (2005) 386–395;
(d) A. Karpfen, in: P. Metrangolo, G. Resnati (Eds.), Halogen Bonding Fundamentals and Applications, Springer, Berlin, 2008, pp. 1–16;
(e) P. Metrangolo, F. Meyer, T. Pilati, G. Resnati, G. Terraneo, Angew. Chem. Int. Ed. 47 (2008) 6114–6127;
(f) G. Cavallo, P. Metrangolo, T. Pilati, G. Resnati, M. Sansotera, G. Terraneo, Chem. Soc. Rev. (2010), doi:10.1039/b926232f.
[4] (a) G. Gattuso, A. Notti, S. Pappalardo, M.F. Parisi, T. Pilati, G. Resnati, G. Terraneo, CrystEngComm 11 (2009) 1204–1206;
(b) A. Dey, P. Metrangolo, T. Pilati, G. Resnati, G. Terraneo, I. Wlassics, J. Fluorine Chem. 113 (2009) 816–823;
(c) A. Abate, S. Biella, G. Cavallo, F. Meyer, H. Neukirch, P. Metrangolo, T. Pilati, G. Resnati, G. Terraneo, J. Fluorine Chem. 113 (2009) 1171–1177;
(d) P. Metrangolo, T. Pilati, G. Terraneo, S. Biella, G. Resnati, CrystEngComm 11 (2009) 1187–1196;
(e) R. Bertani, P. Sgarbossa, A. Venzo, F. Lelj, A. Amati, G. Resnati, T. Pilati, P. Metrangolo, G. Terraneo, Coord. Chem. Rev. 254 (2009) 677–695;
(f) A. Casnati, R. Liantonio, P. Metrangolo, G. Resnati, R. Ungaro, F. Ugozzoli, Angew. Chem. Int. Ed. 45 (2006) 1915–1918;
(g) R. Bertani, E. Ghedini, M. Gleria, R. Liantonio, G. Marras, P. Metrangolo, F. Meyer, T. Pilati, G. Resnati, CrystEngComm 7 (2005) 511–513;
(h) H. Neukirch, E. Guido, R. Liantonio, P. Metrangolo, T. Pilati, G. Resnati, Chem. Commun. (2005) 1534–1536;
(i) S. Biella, G. Gattuso, A. Notti, P. Metrangolo, S. Pappalardo, M.F. Parisi, T. Pilati, G. Resnati, G. Terraneo, Supramol. Chem. 21 (2009) 149–156.

[5] (a) P. Metrangolo, Y. Carcenac, M. Lahtinen, T. Pilati, K. Rissanen, A. Vij, G. Resnati, Science 323 (2009) 1461–1464;
(b) D. Fox, P. Metrangolo, D. Pasini, T. Pilati, G. Resnati, G. Terraneo, CrystEngComm 10 (2008) 1132–1136;
(c) D.W. Bruce, P. Metrangolo, F. Meyer, C. Präsang, G. Resnati, G. Terraneo, A.C. Whitwood, New J. Chem. 32 (2008) 477–482;
(d) E. Cariati, A. Forni, P. Metrangolo, F. Meyer, G. Resnati, S. Righetto, E. Tordin, R. Ugo, Chem. Commun. (2007) 2590–2592;
(e) G. Marras, P. Metrangolo, F. Meyer, T. Pilati, G. Resnati, A. Vij, New J. Chem. 30 (2006) 1397–1402;
(f) E. Guido, P. Metrangolo, W. Panzeri, T. Pilati, G. Resnati, M. Ursini, T.A. Logothetis, J. Fluorine Chem. 126 (2005) 197–207;
(g) R. Bertani, P. Metrangolo, A. Moiana, E. Perez, T. Pilati, G. Resnati, I. Rico-Lattes, A. Sassi, Adv. Mater. 14 (2002) 1197–1201;
(h) A. Farina, S.V. Meille, M.T. Messina, P. Metrangolo, G. Resnati, Angew. Chem. Int. Ed. 38 (1999) 2433–2436.
[6] (a) P. Metrangolo, F. Meyer, T. Pilati, D.M. Proserpio, G. Resnati, Chem. Eur. J. 13 (2007) 5765–5772;
(b) R. Thaimattam, C.V.K. Sharma, A. Clearfield, G.R. Desiraju, Cryst. Growth Des. 1 (2001) 103–106.
[7] (a) K.E. Riley, J.S. Murray, P. Politzer, M.C. Concha, P. Hobza, J. Chem. Theor. Comp. 5 (2009) 155–163;
(b) F.F. Awwadi, R.D. Willet, K.A. Peterson, B. Twamley, Chem. Eur. J. 12 (2006) 8952–8960;
(c) P. Politzer, P. Lane, M.C. Concha, Y. Ma, J.S. Murray, J. Mol. Model. 13 (2007) 305–311;
(d) P. Auffinger, F.A. Hays, E. Westhof, P.S. Ho, Proc. Natl. Acad. Sci. U.S.A. 101 (2004) 16789–16794;
(e) J.S. Murray, M.C. Concha, P. Lane, P. Hobza, P. Politzer, J. Mol. Model. 14 (2008) 699–704;
(f) P. Politzer, J.S. Murray, M.C. Concha, J. Mol. Model. 14 (2008) 659–665;
(g) T. Brinck, J.S. Murray, P. Politzer, Int. J. Quant. Chem.: Quant. Biol. Symp. 19 (1992) 57–64;
(h) W. Wang, N.-B. Wong, W. Zheng, A. Tian, J. Phys. Chem. A 108 (2004) 1799–1805.
[8] R. Bailey Walsh, C.W. Padgett, P. Metrangolo, G. Resnati, T.W. Hanks, W.T. Pennington, Cryst. Growth Des. 1 (2001) 165–175.
[9] R. Liantonio, P. Metrangolo, T. Pilati, G. Resnati, Acta Crystallogr. E 58 (2002) o575–o577.
[10] (a) R. Liantonio, P. Metrangolo, T. Pilati, G. Resnati, Cryst. Growth Des. 3 (2003) 355–361;
(b) R. Liantonio, P. Metrangolo, F. Meyer, T. Pilati, W. Navarrini, G. Resnati, Chem. Commun. (2006) 1819–1820.
[11] J.Y. Lee, S.J. Hong, C. Kim, Y. Kim, Dalton Trans. (2005) 3716–3721.
[12] T. Caronna, R. Liantonio, T.A. Logothetis, P. Metrangolo, T. Pilati, G. Resnati, J. Am. Chem. Soc. 126 (2004) 4500–4501.
[13] M. Eddaoudi, D.B. Moler, H. Li, B. Chen, T.M. Reineke, M. O'Keeffe, O.M. Yaghi, Acc. Chem. Res. 34 (2001) 319–330.
[14] (a) X. Wang, M. Simard, J.D. Wuest, J. Am. Chem. Soc. 166 (1994) 12119–12120;
(b) M.J. Zaworotko, Chem. Soc. Rev. 23 (1994) 283–288;
(c) P. Brunet, M. Simard, J.D. Wuest, J. Am. Chem. Soc. 119 (1997) 2737–2738;
(d) L. Vaillancourt, M. Simard, J.D. Wuest, J. Org. Chem. 63 (1998) 9746–9752;
(e) J.-H. Fournier, T. Maris, J.D. Wuest, W. Guo, E. Galoppini, J. Am. Chem. Soc. 125 (2003) 1002–1006;
(f) P. Grosshans, A. Jouaiti, M.W. Hosseini, N. Kyritsakas, New J. Chem. 27 (2003) 793–797;
(g) S.V. Lindeman, J. Hecht, J.K. Kochi, J. Am. Chem. Soc. 125 (2003) 11597–11606;
(h) K.I. Nättinen, K. Rissanen, Inorg. Chem. 42 (2003) 5126–5134;
(i) K.I. Nättinen, K. Rissanen, Cryst. Growth Des. 3 (2003) 339–353;
(j) H. Sauriat-Dorizon, T. Maris, J.D. Wuest, J. Org. Chem. 68 (2003) 240–246;
(k) K.I. Nättinen, P.E.N. de Bairos, P.J. Seppala, K.T. Rissanen, Eur. J. Inorg. Chem. (2005) 2819–2825;
(l) D. Laliberte, T. Maris, P.E. Ryan, J.D. Wuest, Cryst. Growth Des. 6 (2006) 1335–1340.
[15] G.S. Papaefstathiou, L.R. MacGillivray, Angew. Chem. Int. Ed. 41 (2002) 2070–2073.
[16] The stilbene **A** adopts a bent conformation. The central atoms C7A and C8A are 0.163 and 0.144 Å out of the least-squares mean plane of the whole molecule, and the peripheral atoms I1A and I2A are −0.260 and −0.227 Å out of the same plane. The olefine **B** is also a bit bent, the corresponding distances from the molecular least-squares mean plane being 0.043, 0.166, −0.083 and −0.321 Å.
[17] C.F. Macrae, P.R. Edgington, P. McCabe, E. Pidcock, G.P. Shields, R. Taylor, M. Towler, J. van de Streek, J. Appl. Crystallogr. 39 (2006) 453–457, see also http://www.ccdc.cam.ac.uk/products/mercury/.
[18] L.J. Farrugia, J. Appl. Crystallogr. 30 (1997) 565–566.
[19] The formed networks in co-crystals **5** and **6** were analyzed with the software Topos 4.0 by V.A. Blatov, IUCr CompComm. Newsletter 7 (2006) 4; see also http://www.topos.ssu.samara.ru.
[20] The only interactions significantly shorter than the sum of van der Waals radii are H···F HBs involving fluoroarene and pyridine rings (the shortest being 2.45 Å long) and the N26···C6A($1-x$, $-y$, $1-z$) contact (3.133.(5) Å long).
[21] V.A. Blatov, L. Carlucci, G. Ciani, D.M. Proserpio, CrystEngComm 16 (2004) 377–395.
[22] M.C. Burla, M. Camalli, B. Carrozzini, G.L. Cascarano, C. Giacovazzo, G. Polidori, R. Spagna, J. Appl. Crystallogr. 36 (2003) 1103–1112.
[23] G.M. Sheldrick, SHELXL-97 1997, Program for the Refinement of Crystal Structures, University of Göttingen, German.